ORIGINAL ARTICLE

Compression Tests on Large Angle Columns in High Strength Steel

Marios-Zois Bezas, Jean-François Demonceau[1], Ioannis Vayas[2], Jean-Pierre Jaspart[1]

Correspondence

Mr. Marios-Zois Bezas
University of Liege
Steel and Composite Construction
Allée de la Découverte 9 B52/3
Liege 4000, Belgium
Email: Marios-Zois.Bezas@uliege.be

Abstract

The paper discusses the stability behaviour of large angle columns in high strength steel subjected to compression loads. It presents a number of compression tests on such columns that have been performed at University of Liege with different eccentricities and slenderness and, as a result, different buckling failure modes observed. The experimental campaign is intended to widen the knowledge about the behaviour of high strength steel columns with large angle sections in compression and bending and so to complement previous experimental studies. The tests have been accompanied by numerical analyses and calculations of the load carrying capacities through present Eurocode prescribed methods. The numerical simulations have been carried out by application of the FEM software FINELG using beam elements and considering of relevant imperfections as well as geometrical and material non – linearities. The numerical and analytical results are compared and validated with the corresponding experimental ones and summarized in the present paper. The experimental campaign and the numerical simulations are part of the European-funded RFCS project ANGELHY "Innovative solutions for design and strengthening of telecommunications and transmission lattice towers using large angles from high strength steel and hybrid techniques of angles with FRP strips".

Keywords

Stability, High strength steel, Angle cross-sections, Buckling, Finite elements analysis

1 Introduction

Angles have been used since the very beginning of steel construction due to their easy transportation and on-site erection. They are extensively used in lattice towers and masts for telecommunication or electricity transmission and, in a wide range of civil engineering applications including buildings, bridges; but also, for the strengthening of existing structures. Recent developments have led to a wider application of large angle sections made of high strength steel, but there is a lack of consistent European rules for the design of members made of such angle profiles.

To widen the knowledge about the stability behaviour of steel columns from angle cross-sections subjected to compression and bending, twelve (12) buckling tests on columns with large angle steel profiles have been performed. The experiments have been limited to S460M high strength steel only, given the fact that a number of compression tests on angles with lower steel grades have already been performed before by NTUA [1], as well as in Tsinghua University of Beijing [2]. The test campaign has been realized at the "Laboratoire de Mécanique des Matériaux et Structures" of Liège University.

The selection of the specimens, the details about the experimental campaign such as measurements before and during the tests, as well as the test results, are presented in this article. A comparison of the results obtained through the experiments and numerical simulations, considering relevant imperfections as well as geometrical and material non-linearities, has been achieved by the full non-linear finite element software FINELG, using beam elements. Finally, a comparison of the obtained test results and the Eurocode predictions has been done. The experimental campaign and the numerical simulations are part of the European-funded RFCS project ANGELHY [3].

2 Details of test specimens

For the experimental campaign, two profiles from large angle cross-sections made of high strength steel have been selected. For each profile, six column tests have been performed with three different lengths per profile and with two positions of load application for each length. The points of load application selected (see Figure 1) are: the centre of gravity (G), which corresponds to pure compression in the angle and the middle of the wall (P_2), which is the most

[1] University of Liege, Liege, Belgium.
[2] National Technical University of Athens, Athens, Greece.

usual connection point for angles in structures (position of the connecting bolt).

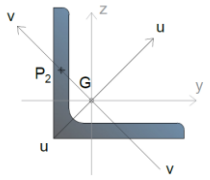

G centre of gravity
P_2 the middle of the wall
u-u major principal axis (weak axis displacement)
v-v minor principal axis (strong axis displacement)
y,z geometrical axes

Figure 1 Position of applicable load and axis definition

Table 1 summarizes all the details about the specimens. The name of each specimen consists of two numbers Sp## (e.g. Sp13):

- the first number indicates the profile: 1 for L150x150x18 and 2 for 200x200x16;
- the second one is the serial number of the specimen (1 to 6 per profile).

Table 1 Details about the specimens

ID of Specimen	Profile	Steel grade	Length [mm]	Eccentricity [mm]
Sp11	L 150x150x18	S460M	2500	0,00
Sp12	L 150x150x18	S460M	2500	e_v = 48,74
Sp13	L 150x150x18	S460M	3000	0,00
Sp14	L 150x150x18	S460M	3000	e_v = 48,74
Sp15	L 150x150x18	S460M	3500	0,00
Sp16	L 150x150x18	S460M	3500	e_v = 48,74
Sp21	L 200x200x16	S460M	3000	0,00
Sp22	L 200x200x16	S460M	3000	e_v = 66,64
Sp23	L 200x200x16	S460M	3500	0,00
Sp24	L 200x200x16	S460M	3500	e_v = 66,64
Sp25	L 200x200x16	S460M	4000	0,00
Sp26	L 200x200x16	S460M	4000	e_v = 66,64

For all tests, constant dimensions have been selected for the end plates welded at the extremities of the angle members, in order to simplify the placement procedure of the specimen in the test rig. The advantage of this decision is that the bolts and the position of the applied load is always the same for the machine and the eccentricity introduced by moving the profile on the end plates. The steel grade of the end plates is S355. Figure 2 shows details of the specimen's end plates.

The welds have been designed according to EN1993 – 1 – 8 [4]. The welding lengths are shown in Figure 2 and include all the straight sides of the cross-sections. For all the specimens, the minimum required weld thickness is 6 mm, except for specimens Sp11 and Sp21 which require a minimum thickness of 8 mm.

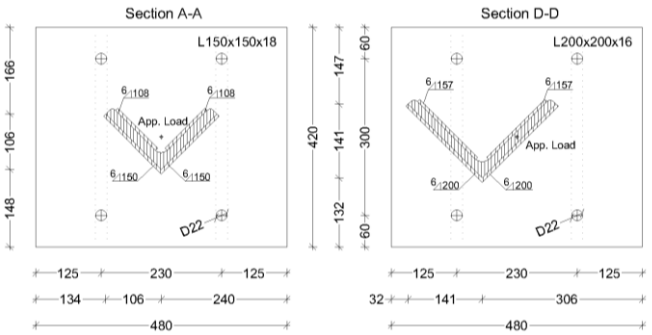

Figure 2 Detail of end plates in case of centrally (left) and eccentrally (right) load specimens

3 Measurements before and during a test

The tests have been performed with the Amsler 500 testing machine (see Figure 3) which is able to apply a compression load up to 5000 kN.

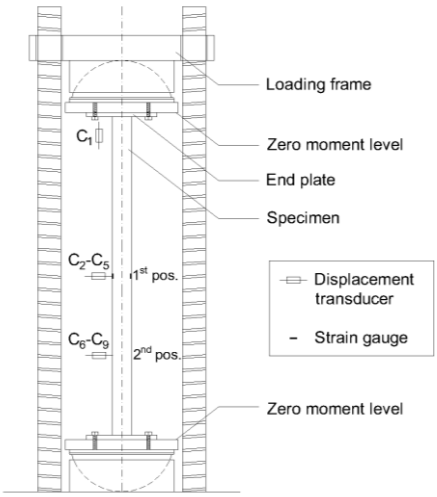

Figure 3 Sketch of Amsler 500 test machine

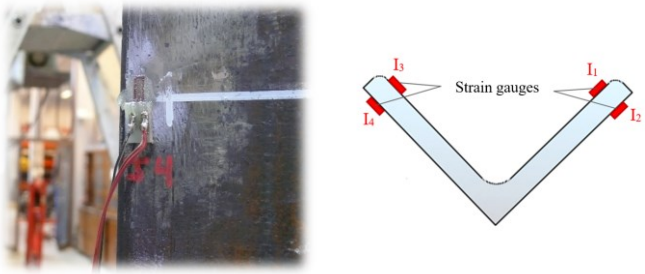

Figure 4 Strain gauges positions at the mid-height cross-section

Four strain gauges (I_1 to I_4) have been placed at the mid-height cross-section of each column as shown in Figure 4, in order to check the local yielding. The strain gauges have been placed as closer as possible to the edges of the legs of the cross-section, taken into account the curvature of the edges.

3.1 Actual dimensions of the cross-sections

The actual geometrical dimensions of each angle section – the width (b_i) and the thickness (t_i) of each leg – have been measured at 3 points along the member length: 1/4, 1/2 and 3/4 of the total length (L). The mean values of the measurements are reported in Table 2 below.

Table 2 Measurements of the actual dimensions of the cross-sections

ID of Specimen	Length [mm]	b_1 [mm]	b_2 [mm]	t_1 [mm]	t_2 [mm]
Sp11	2500	149,97	150,09	18,16	18,14
Sp12	2500	150,07	150,12	18,18	18,04
Sp13	3000	150,11	149,92	18,04	18,16
Sp14	3000	150,09	150,10	18,04	18,17
Sp15	3500	150,07	150,11	18,17	18,07
Sp16	3500	150,11	149,95	18,16	18,19
Sp21	3000	200,31	200,41	16,32	16,34
Sp22	3000	200,36	200,39	16,39	16,29
Sp23	3500	200,25	199,92	16,32	16,28
Sp24	3500	200,05	200,01	16,42	16,10
Sp25	4000	199,96	200,27	16,33	16,35
Sp26	4000	200,06	200,39	16,32	16,31

$b_i=1/3(b_i^{L1/4}+b_i^{L1/2}+b_i^{L3/4})$ (i=1,2) ; $t_i=1/3(t_i^{L1/4}+t_i^{L1/2}+t_i^{L3/4})$ (i=1,2)

3.2 Initial Imperfections

Two measurements (M1 & M2) on each external face and along the column length have been performed so as to evaluate the initial deformation of the specimens. Figure 5 shows the details of the set-up configuration. Due to the end plates and the measurement system itself, it wasn't possible to take measurements quite close to the ends of the specimens. As a result, all the measurements start 140 mm after the top end plate and finish 140 mm before the bottom one. A measurement has been taken every 50 mm along the column. It is quite reasonably assumed that the columns close to the end plates (140 mm) are straight.

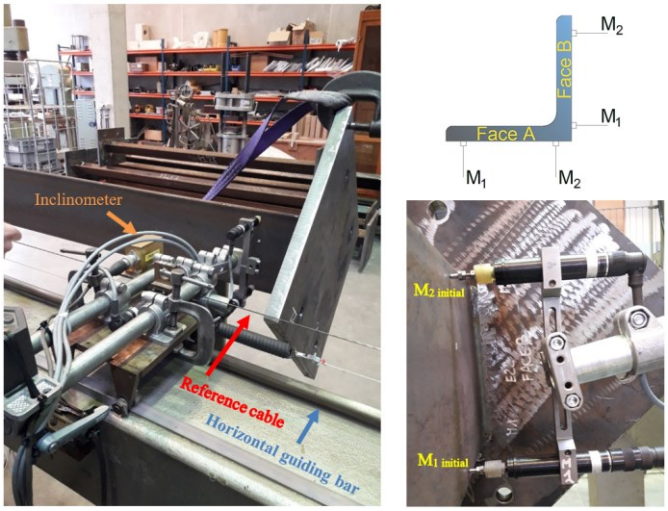

Figure 5 Measurement system for geometrical imperfections (left), detail and position of the displacement transducers (right)

An accurate comparison between the actual measured imperfections of the specimens and those assumed in the Eurocode is quite difficult to do. The European norm EN 1090-2 [5] prescribes that the deviation from straightness should be Δ ≤ L[mm]/750 while in prEN 1993-1-14 [6] it is stated that 80% of the geometric fabrication tolerances given in [5] should be applied. This leads to an initial bow imperfection of magnitude approximately equal to L[mm]/1000 and usually a deformation shape similar to the first member instability mode is assumed, while in reality the shape is more complex. However, through a rough check of the values, it can be concluded that measured imperfections were smaller for all specimens than the geometrical tolerances prescribed in European regulations and so the specimens were quite straight.

3.3 Material properties

Coupon tests have been performed in accordance with ISO 6892-1:2016 [7]. The samples have been extracted from one of the extremities of the angle member (see Figure 6) after the buckling tests as recommended in ISO 377:1997 [8]. Figure 7 shows the strain – stress curves obtained from those tensile tests and Table 3 the characteristic values of the mechanical properties. The yield stress fy is determined by the value of the plateau of the curves.

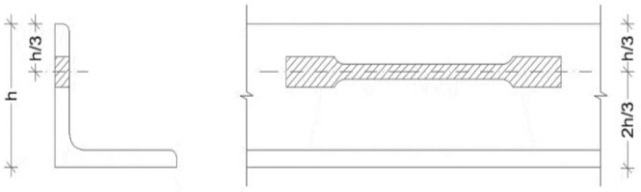

Figure 6 Location of tensile samples for coupon tests based on [9]

Table 3 Coupon test's results

No	ID of material	E [MPa]	Yielding stress f_y [MPa]	Ultimate stress f_{ult} [MPa]	Characterized specimens
1	S 460/1	203155	425,8	572,50	Sp12, Sp13, Sp14, Sp15, Sp16
2	S 460/2	208947	487,6	604,64	Sp21, Sp22, Sp23, Sp25, Sp26
3	S 460/3	197317	417,2	560,87	Sp11
4	S 460/4	203797	472,6	587,21	Sp24

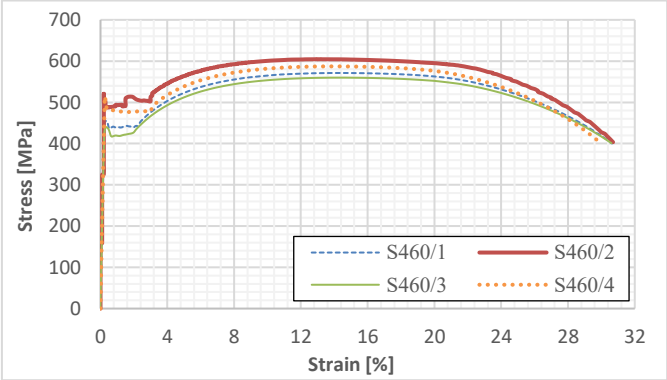

Figure 7 Strain-stress curves from the coupon tests

3.4 Measurements during the test

During the tests, following displacements illustrated in Figure 8 were measured:

– the vertical displacement C_1;
– four horizontal displacements C_2, C_3, C_4 and C_5 at the mid cross-section (1st position);
– four horizontal displacements C_6, C_7, C_8 and C_9 at the lower cross-section (2nd position).

All the displacement transducers have been placed 30 mm from the edges/corner of all cross-sections and profiles. The configuration of the test rig allowing to record those displacements, is shown in Figure 9.

In addition, strains at four points of the cross-section at mid-height of the columns, as shown in Figure 4, were measured.

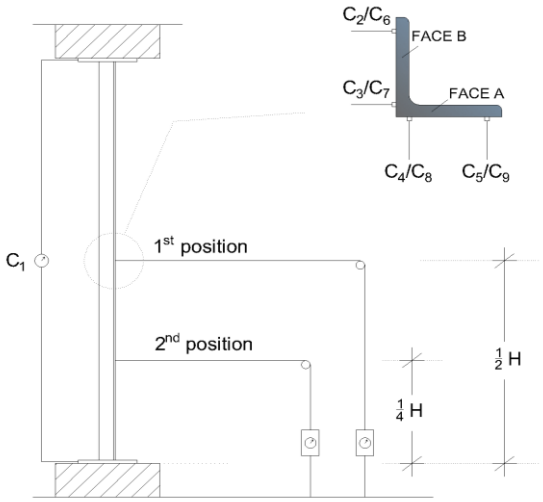

Figure 8 Measurements during a test (H is the height of the specimen)

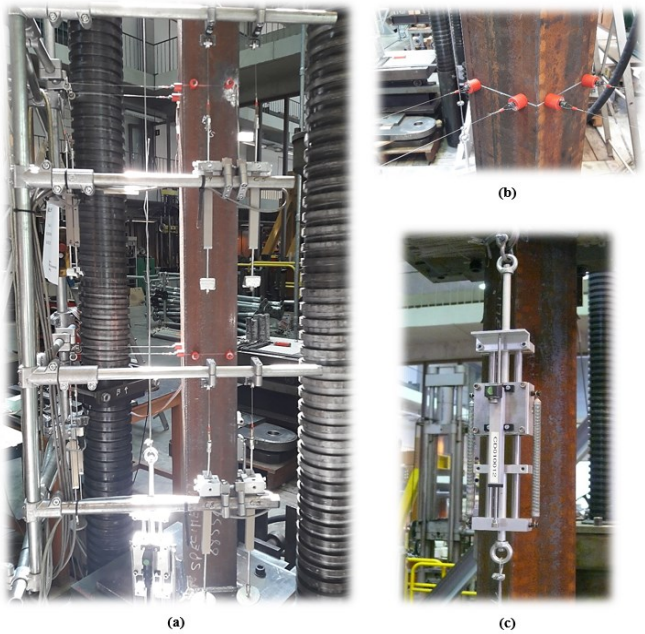

Figure 9 (a) General view of test rig with the measurement devices, (b) Connection points of displacement transducers on the cross-section and (c) Vertical displacement transducer

4 Results, comparisons and discussion

The results of the tests are presented below through graphs and tables. All the results (initial imperfections, deflections, strains, twists) can be found in [9]. Numerical simulations of the experimental tests with FINELG have been performed, by taking into account the actual dimensions, lengths, imperfections and material properties. A comparison between the ultimate resistance obtained by the tests and through EN1993-1-1 [10] predictions has also been achieved for centrally loaded columns.

4.1 Results of the experimental tests

Figure 10 and Figure 11 show the axial displacement versus the applied load for profiles L150x150x18 and L200x200x16 respectively. Due to the lack of perfectly connections of the end plates, some specimens appeared to be more flexible in the beginning of the test. However, this was corrected, and the corrected curves are illustrated in both figures. More details about the correction can be found in [9].

Figure 10 and Figure 11 indicate, that the results obtained for the tests are in line with the physical expectations (for instance, the influence of the member length and of the eccentricity on the member stiffness and resistance properties). This seems a priori to validate the initial selection of the different parameters in the test campaign.

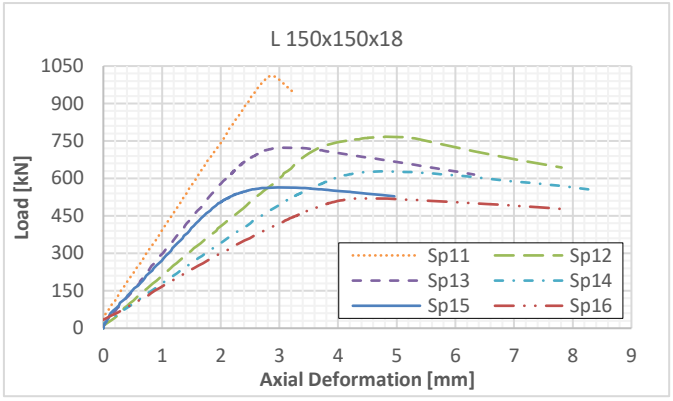

Figure 10 Load vs axial deformation of tested profiles L 150x150x18

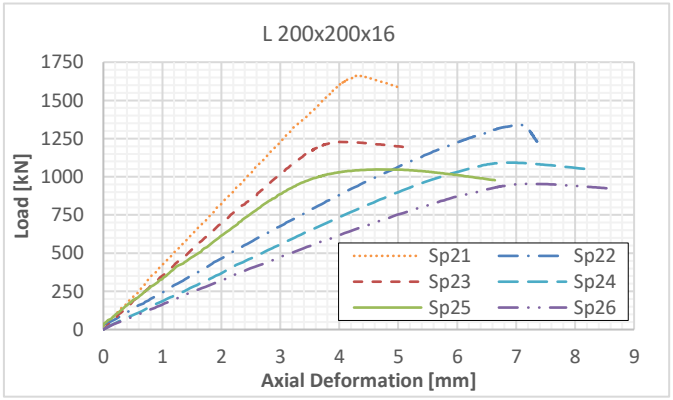

Figure 11 Load vs axial deformation of tested profiles L 200x200x16

For all centrally loaded tests, the deflections along the weak axis increased significantly with the load until failure be reached by weak axis buckling. Specimens Sp11, Sp13 and Sp15 failed in a pure flexural buckling mode, while in specimens Sp21, Sp23 and Sp25 twist rotations were recorded, and in addition to weak axis deflections indicating a flexural torsional buckling mode.

The eccentrically loaded specimens were subjected initially to compression and strong axis bending. However, at larger load levels their tendency to buckle towards the weak axis lead them to deflect towards both principal axes. In the specimens Sp22, Sp24 and Sp26 these deflections were accompanied by significant twist rotations clearly indicating failure with a flexural-torsional buckling mode. On the contrary, twist rotations were small for specimens Sp12, Sp14 and Sp16 indicating a mixed mode between flexural and flexural torsional buckling.

Local buckling was not visibly observed in any specimen.

4.2 Comparison with numerical simulations

A comparison of the stiffness and the ultimate resistance of the members obtained through the experiments and the numerical models, considering relevant imperfections as well as geometrical and material non-linearities is presented below.

The numerical analyses of the test specimens have been performed with the FINELG [11] non-linear finite element software using beam elements with 6DOF, given the fact that no local buckling took place during the tests. The FEM nodes are located at the centre of gravity of the angle cross-section, while the "fictitious" node 22 is used only for the orientation of the beam elements (see Figure 12). Only the column has been simulated while the end plates have been considered indirectly. The columns are assumed as pin-end members (as in the test rig) with free rotations at their extremities, except the rotation which leads to torsion that is blocked. To evaluate the actual critical length of the specimen, 107 mm (thicknesses of end plates of specimens and machine plates) was added to the length of all specimens.

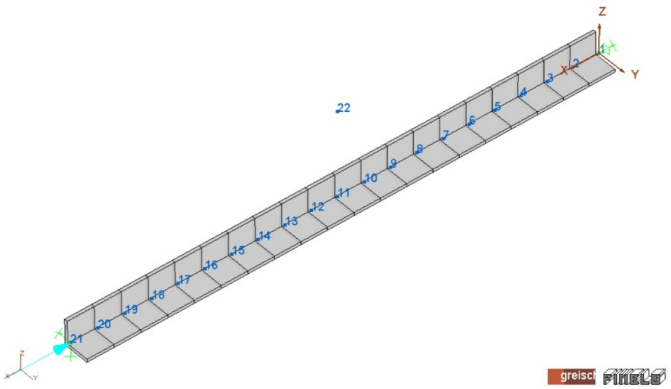

Figure 12 FEM model used for the numerical simulations

The FINELG finite element analyses adopting the GMNIA method were performed, considering:

- an initial member imperfection with shape and magnitude in accordance with the measured ones;
- residual stresses which result from the hot-rolling procedure; the pattern is shown in Figure 13. The selected pattern is issued from previous studies [12], in which appropriate measurements had been realized; this pattern is a rather a common one;
- a material law in accordance with the measured ones (Figure 7).

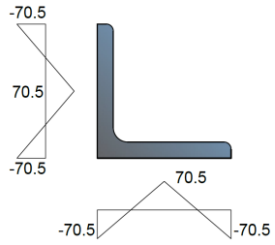

Figure 13 Assumed distribution of residual stresses

A tolerance on the position of the applying load up to 2,0 mm has been also adopted for the numerical simulations. It has been found that even a small eccentricity could affect the ultimate resistance in comparison to the perfect "no loading eccentricity" case. The influence of this small eccentricity of the applying load on the stiffness and the ultimate resistance has been also observed in [13]. For example, an eccentricity equals to 1,5mm is able to change the ultimate resistance by close to 6% for the specimens Sp2#. This tolerance could be explained by the two following reasons:

- the position of the load has been designed to be at the centre of the end plates and in such a way that the point coincides with the centre of gravity of the cross section. But in reality, due to small differences of the cross-section geometry, the real centre of gravity does not coincide exactly with the point of loading;
- the positioning of the specimen in the testing rig may also induce a small and unexpected eccentricity.

Table 4 Comparison between ultimate resistances obtained through tests and finite element models

ID of Specimen	Profile	P_{exp} [kN]	P_{FEM} [kN]	P_{exp}/P_{FEM}
Sp11	150x150x18	1010,6	1028,6	0,98
Sp12	150x150x18	767,3	774,1	0,99
Sp13	150x150x18	723,2	739,3	0,98
Sp14	150x150x18	628,3	645,9	0,97
Sp15	150x150x18	563,9	575,9	0,98
Sp16	150x150x18	519,8	536,0	0,97
Sp21	200x200x16	1661,5	1690,6	0,98
Sp22	200x200x16	1341,4	1361,0	0,99
Sp23	200x200x16	1228,0	1267,4	0,97
Sp24	200x200x16	1092,3	1107,6	0,99
Sp25	200x200x16	1048,1	1082,2	0,97
Sp26	200x200x16	953,6	959,1	0,99

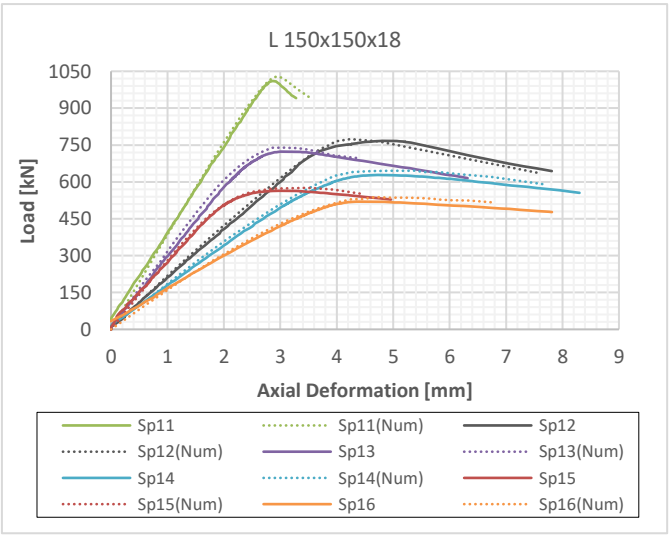

Figure 14 Comparison between test and FEM results for Sp1#

Figure 14 and Figure 15 compare the experimental response of each specimen with the numerical one obtained through FEM, and the results are reported also in Table 4. It is obvious that there is a very good agreement between the numerical simulations and the experimental results in terms of stiffness and ultimate resistances (less

than 3%).

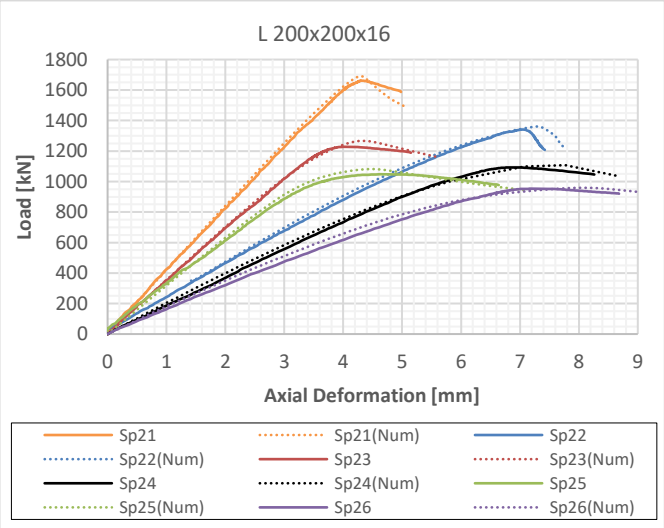

Figure 15 Comparison between test and FEM results for Sp2#

4.3 Comparison with Eurocode predictions

According to EN1993-1-1 the first profile (L 150x150x18) is classified as Class 1 and the second one (L 200x200x16) as Class 4. The procedure of EN1993-1-5 [14] has been followed to evaluate the effective cross-section of the Class 4 profiles and the reduction factors for the area equal to β=0,845 (for Sp21 & Sp25) and β=0,837 (Sp23) have been obtained. Even if, as already said, no plate buckling has been reported during the tests.

Figure 16 presents the experimental results (only for centrally loaded specimens) compared with those obtained through the present recommendations of EN1993-1-1; reference buckling curves a_0, a and b are reported too.

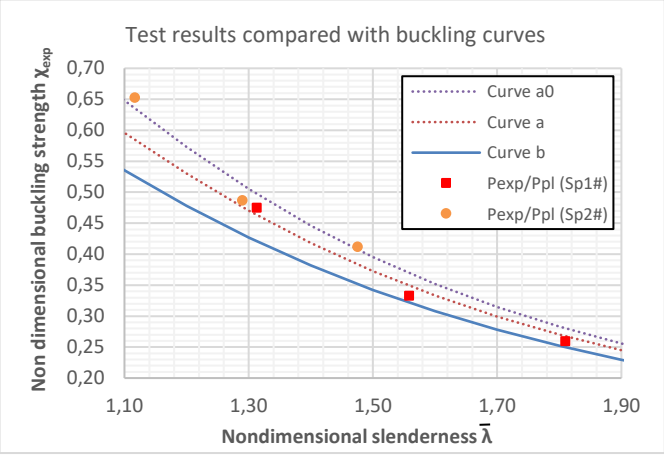

Figure 16 Comparison of experimental results with buckling curves of EN1993-1-1

The buckling reduction factor χ_{exp} of specimens has been calculated by the equation (1):

$$\chi_{exp} = \frac{P_{ult}}{P_{pl}} = \frac{P_{ult}}{\beta \cdot A \cdot f_y} \quad (1)$$

and the nondimensional slenderness $\bar{\lambda}$ has been obtained by:

$$\bar{\lambda} = \sqrt{\frac{N_{pl}}{N_{cr}}} \quad (2)$$

where N_{cr} is the elastic critical load for the relevant buckling mode (i.e. the minimum eigen value of associated to all flexural and flexural-torsional modes) obtained through an elastic instability analysis considering actual material and gross cross-section properties using FINELG software. A pure torsional mode cannot be obtained for a centrally loaded angle column as explained in [15]. The actual yielding stress f_y has been used for the calculations. Table 5 includes the results from the calculations indicated in Figure 16 as well as the ultimate resistance calculated by EN1993-1-1.

Table 5 Nondimensional slenderness $\bar{\lambda}$ and reduction factor χ calculations

Sp##	N_{cr} [kN]	$\bar{\lambda}$ [-]	P_{pl} [kN]	P_{EC3} [kN]	P_{exp}/P_{EC3}	$\chi_{exp}=P_{exp}/P_{pl}$
Sp11	1233,7	1,31	2128	894,8	1,13	0,475
Sp13	894,3	1,56	2172	698,5	1,04	0,333
Sp15	663,6	1,81	2174	542,7	1,04	0,260
Sp21	2040,9	1,12	2546	1337,2	1,24	0,653
Sp23	1515,1	1,29	2522	1088,6	1,13	0,487
Sp25	1168,6	1,48	2545	894,1	1,17	0,412

In Eurocode 3, the buckling curve b has been selected for axially loaded equal angle columns (solid line in Figure 16). It has been found that the experimental results are in line with this curve or above. Furthermore, it can be easily observed that the actual ultimate resistance of all centrally load columns is higher than the predictions of Eurocode; the latter seems so to provide safe evaluations (see Table 5), especially for specimens Sp2# where the detrimental effects of local buckling are possibly overestimated.

5 Conclusions

In the current paper the stability of steel columns with large angle high strength steel profiles has been investigated through twelve (12) buckling tests. From this experimental program and the accompanying numerical/analytical studies, following conclusions may be drawn:

- The centrically loaded specimens with class 1 cross-section (Sp11, Sp13, Sp15) and the eccentrically loaded specimens with class 4 cross-section (Sp22, Sp24, Sp26) failed very clearly in a pure weak axis flexural buckling mode and correspondingly flexural-torsional buckling mode.
- The centrically loaded specimens with class 4 cross-section (Sp21, Sp23, Sp25) and the eccentrically loaded specimens with class 1 cross-section (Sp12, Sp14, Sp16) failed more or less in a flexural-torsional buckling mode, which was more pronounced in the former.
- Local buckling was not visible observed at any specimen, although one of them was categorized as class 4 according to EN1993-1-1.
- A very good agreement between numerical GMNIA simulations and experimental results in terms of stiffness and ultimate resistances has been achieved.
- A small eccentricity of the position of the applying load can affect the ultimate resistance of the member in comparison with the perfect "no loading eccentricity" case. For the current study, an eccentricity equal to 1,5 mm may reduce the ultimate resistance by about 6%.
- The design resistance of the specimens based on EN1993-1-1

and EN1993-1-5 is on the safe side, especially for the second profile for which the local buckling reduction effects seem to be overestimated by Eurocode.

Acknowledgment

The work presented here is carried in the framework of a European Research project entitled ANGELHY "Innovative solutions for design and strengthening of telecommunications and transmission lattice towers using large angles from high strength steel and hybrid techniques of angles with FRP strips", with a financial grant from the Research Fund for Coal and Steel (RFCS) of the European Community. The authors gratefully acknowledge this financial support.

References

[1] Spiliopoulos A, Dasiou M-E, Thanopoulos P, Vayas I, *Experimental tests on members made from rolled angle sections*, Steel Construction – Design and Research, Vol.11, Issue 1, pp. 84-93, 2018.

[2] Ban H.Y, Shi G, Shi Y.J, Wang Y.Q, *Column buckling tests of 420MPa high strength steel single equal angles*, International Journal of Structural Stability and Dynamics, Vol.13, 2013.

[3] Vayas I, Jaspart JP, Bureau A, Tibolt M, Reygner S, Papavasiliou M, *Telecommunication and transmission lattice towers from angle sections- the ANGELHY project*, Eurosteel2020.

[4] EN1993-1-8 (2005). *Design of steel structures. Part 1-8 Design of joints*. Brussels. Comité Europeen de Normalisation (CEN).

[5] ISO 1090-2: *Technical requirements for the execution of steel structures*, Comité Europeen de Normalisation (CEN), 2008.

[6] prEN1993-1-14 (20XX): XXXX, Brussels. Comité Europeen de Normalisation (CEN).

[7] ISO 6892 – 1: *Metallic materials – Tensile testing – Part 1: Method of test at room temperature*, Brussels, Comité Europeen de Normalisation (CEN), 2016.

[8] EN ISO 377: *Steel and steel products — Location and preparation of samples and test pieces for mechanical testing*, Brussels, Comité Europeen de Normalisation (CEN), 1997.

[9] Bezas MZ, Jaspart JP, Demonceau JF, Labeye N, *Report about the compression tests on large angle columns in high strength steel*, RFCS ANGELHY project, University of Liege, 2020.

[10] EN1993-1-1 (2005). *Design of steel structures. Part 1-1 General rules and rules for buildings*, Brussels, Comité Europeen de Normalisation (CEN).

[11] FINELG: *Non-linear finite element analysis program*, *User's manual*, Version 9.0, Greisch Ingeniere, 2003.

[12] Zhang L, Jaspart JP, *Stability of members in compression made of large hot-rolled and welded angles*, Université de Liège, 2013.

[13] de Menezes AA, da S. Vellasco PCG, de Lima LRO, da Silva AT, *Experimental and numerical investigation of austenitic stainless steel hot-rolled angles under compression*, Journal of Constructional Steel Research, Vol.152, pp. 42-56, 2019.

[14] EN1993-1-5 (2006). *Design of steel structures. Part 1-5 Plate structural elements*, Brussels, Comité Europeen de Normalisation (CEN).

[15] de Ville de Goyet V (1989), *L'analyse statique non linéaire par la méthode des éléments finis des structures spatiales formées de poutres à section non symétrique*, PhD thesis, University of Liège.